Publishing House
AKAPIT

COMPUTER METHODS IN MATERIALS SCIENCE

Informatyka w Technologii Materiałów

Vol. 16, 2016, No. 4

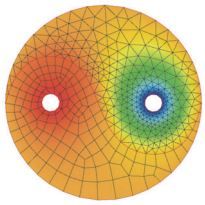

COMPUTER AIDED DESIGN OF MANUFACTURING OF AUTOMOTIVE PART MADE OF MAGNESIUM ALLOY

MATEUSZ AMBROZIŃSKI[1], ŁUKASZ RAUCH[1]*, MAREK PAĆKO[1], ZBIGNIEW GRONOSTAJSKI[2], KAROL JAŚKIEWICZ[2], WŁADYSŁAW CHORZĘPA[3]

[1]AGH University of Science and Technology, al. Mickiewicza 30, 30-059 Kraków, Poland
[2]Politechnika Wrocławska, ul. Łukasiewicza 5, 50-371 Wrocław, Poland
[3]Kirchhoff Polska Sp. z o.o., ul. Wojska Polskiego, 39-300 Mielec, Poland
**Corresponding author: lrauch@agh.edu.pl*

Abstract

Evaluation of the possibility of substitution of steel part in the car body by the one made of AZ31 alloy was the objective of the paper. Bracket in the support of the steering wheel was selected for the analysis. Two criteria were selected to evaluate the possibility of using the Mg alloy part: i) stiffness of this part cannot be lower than that of the steel part, ii) Manufacturing of the part has to be possible. The objective of the research was a design of the shape of the bracket, that meets assumed criteria including manufacturing and assembly possibilities. The optimization task was formulated to reach this objective. Maximum stiffness of the part was the objective function and technological limitations were the constraints. Dimensions of the bracket were the optimization variables. Optimal shape was designed and numerical simulations were performed to evaluate possibility of stamping of this part. Simulations have shown that the decrease of the thickness is within of acceptable limits and that the strains are below the limiting strains. Thus, proposition of the shape of the magnesium alloy bracket, which can be safely manufactured by stamping, is the main output of the paper.

Key words: Magnesium alloys, stamping, automotive parts, computer aided design

1. INTRODUCTION

The growing interest of using the lightweight structural materials, with satisfactory mechanical properties, makes the scientific and research centres to develop accurate methods of design forming processes, for which the most important are data collected during real experiments, allowing for the correct development of production technology. Magnesium alloys are an example of such a material, successfully used for many years in various fields of industry, including automotive industry (Blawert et al., 2004; Kulekci, 2008; Kawalla et al, 2008a; Musfirah & Jaharah, 2012; Sameer Kumar et al., 2015; Kawalla et al., 2008b). In recent years, the role of magnesium and its alloys as particularly useful construction materials has rapidly increased. Numerous publications dealing with investigation of plastic forming of these alloys can be found in the scientific literature (eg. Kawalla et al., 2006; Hadasik et al, 2009; Ullmann et al., 2012, Kuc et al., 2012; Kuc et al., 2013; Kuc et al., 2014). The most important advantageous features are low density of magnesium alloys and their reasonably low price. Furthermore, the continuous improvement of material and technical properties of magnesium alloys enables the improvement of forming methods of finished products.

It is worth to note, that design of technology of finished products manufacturing from magnesium alloys, particularly alloys for plastic forming, faces a number of problems related to the phenomena that inhibit processes of sheet metal forming. The main aim of the present work was to develop guidelines necessary to design the stamping technology of bracket made from magnesium alloy AZ31, which is

 ISSN 1641-8581

part of the assembly of the cross beam in a passenger car. The particular objectives of the work were twofold. The first was design of the part made of the magnesium alloy to obtain stiffness similar to the steel part. The second was analysis of possible manufacturing of this bracket by stamping.

2. MODEL

Stamping process was simulated in the program Abaqus. Tools shapes have been adopted on the basis of documentation from one of the manufacturers of automotive parts. The material data of sheets made from magnesium alloy AZ31 containing 2.5-3.5%Al, 0.7-1.3%Zn, 0.2-1.3%Mn and balance of Mg, were determined experimentally for a specific temperature in the range of 20 to 400°C. Investigated alloy is characterised by increased strength obtained by specific heat treatment. Good workability at elevated temperatures, low density, good corrosion resistance, machinability and weldability are important advantageous features of this material. AZ31 is non-magnetic and has good thermal and electrical conductivity. Hot deformation of this alloy allows to obtain complicated shapes of products, what makes this material interesting for the automotive industry. Basic physical properties of AZ31 are: density ρ = 1.800 g/m^3, heat expansion coefficient α = 26.8×10^{-6} 1/°C, specific heat c_p = 1040 J/kg°C, heat conductivity k = W/mK, electrical resistivity 92 nΩm, Young modulus 45×10^3 MPa, Poisson coefficient 0.35, melting temperature T_m = 566–632°C.

Plastic deformation of the AZ31 alloy was investigated in numbers of publications, eg. Kuc and Pietrzyk (2010) performed the uniaxial compression tests for this alloy on the Gleeble 3800 thermomechanical simulator. In the present work tensile tests were carried out as more relevant for application to modelling of the stamping process. Zwick machine with the maximum load of 100 kN was used in the tests. The tests were performed in the temperature range 20-350°C and for the strain rates of 10^{-3} and 10^{-1} 1/s.

Typical registered plots of engineering stress vs elongation are shown in figure 1a. The curves do not show physical yield point and the proof stress values $R_{0.2}$ were determined. The slope of the curve in the range between 10 MPa and 60-70% of maximum stress was determined. In this range the relationship was linear. Following this a crossing point between the parallel line at the strain 0.002 and the registered plot was determined and this point was sued as a proof stress. The same algorithm was used to determine longitudinal Young modulus. Average values of the proof stress, ultimate tensile stress, Young modulus and elongation were calculated on the basis of measurements performed for several samples (Ambroziński et al., 2016).

To eliminate the influence of changes of the sample cross section, the inverse analysis proposed in (Szeliga et al., 2005) was applied to obtain true stress – true strain curve. In the first approach inverse analysis yielded this relation in a tabular form and these results are shown in figure 1b. It is seen that the effect of necking on the results was eliminated. In the second step of the inverse analysis coefficients in the equation describing flow stress as a function of strain, strain rate and temperature were the design variables. Various equations were analysed and it was observed that simple equations are not capable to describe the flow stress in a wide range of temperatures and strain rates. Finally the equation proposed by Sellars and McTeggart (1972) was selected:

$$\sigma_p = \sigma_0 + \left(\sigma_{ss(e)} - \sigma_0\right)\left[1 - \exp\left(-\frac{\varepsilon}{\varepsilon_r}\right)\right]^{\frac{1}{2}} - R \tag{1}$$

$$R = \begin{cases} 0 & \varepsilon \le \varepsilon_c \\ \left(\sigma_{ss(e)} - \sigma_{ss}\right)\left[1 - \exp\left(-\left[\dfrac{\varepsilon - \varepsilon_c}{\varepsilon_{xr} - \varepsilon_c}\right]^2\right)\right] & \varepsilon > \varepsilon_c \end{cases}$$

$$\sigma_0 = \frac{1}{\alpha_0}\sinh^{-1}\left(\frac{Z}{A_0}\right)^{\frac{1}{n_0}},$$

$$\sigma_{ss} = \frac{1}{\alpha_{ss}}\sinh^{-1}\left(\frac{Z}{A_{ss}}\right)^{\frac{1}{n_{ss}}},$$

$$\sigma_{sse} = \frac{1}{\alpha_{sse}}\sinh^{-1}\left(\frac{Z}{A_{sse}}\right)^{\frac{1}{n_{sse}}}$$

$$Z = \varepsilon \exp\left(\frac{Q_{def}}{RT_{def}}\right)$$

$$\varepsilon_r = \frac{1}{3.23}\left[q_1 + q_2\left(\sigma_{ss(e)}\right)^2\right],$$

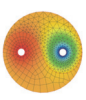

$$\varepsilon_{xr} - \varepsilon_c = \frac{\varepsilon_{xs} - \varepsilon_c}{1.98},$$

$$\varepsilon_c = C_c \left(\frac{Z}{\sigma_{ss(e)}^2} \right)^{N_c},$$

$$\varepsilon_{xs} - \varepsilon_c = C_x \left(\frac{Z}{\sigma_{ss(e)}^2} \right)^{Nx}$$

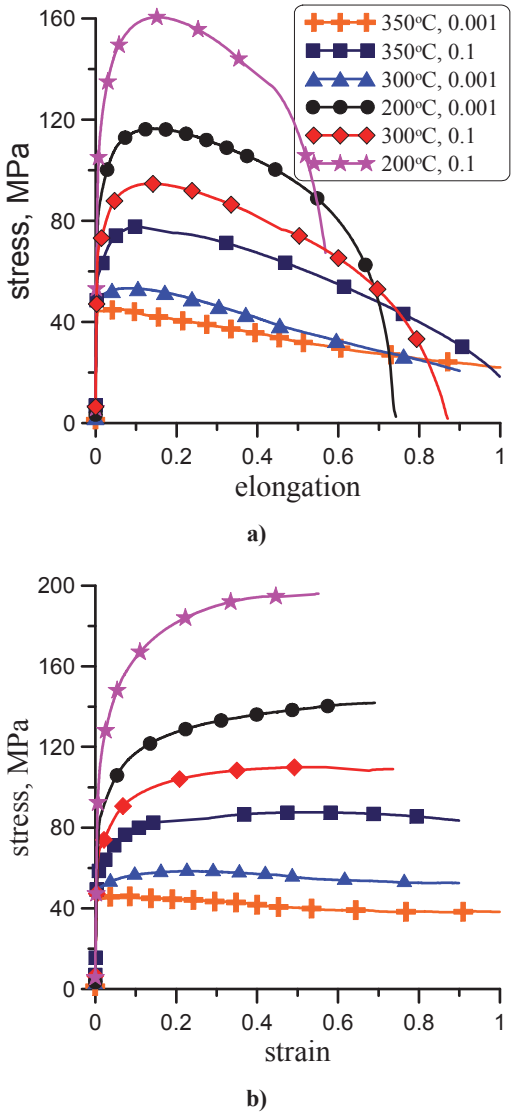

Fig. 1. *Selected results of tensile tests (a) and flow stress after inverse analysis.*

Table 1. *Coefficients in equation (1) obtained from the inverse analysis of tensile tests.*

α_0	α_{sse}	α_{ss}	n_0	n_{sse}	n_{ss}	A_0	A_{sse}
0.4×10^{14}	154	0.0188	0.362×10^{13}	6.796	0.0083	0.125×10^{14}	8.42
A_{ss}	q_1	q_2	C_c	N_c	C_x	N_x	Q_{def}
0.0093	0.332	0	0.0733	0.0378	0.00106	0.4066	149340

Equation (1) contains 16 coefficients, which were determined for the investigated alloy in the temperature range 200°C – 350°C and at strain rates 0.001 and 0.1 s^{-1}. The values of coefficients obtained for the AZ31 alloy are given in table 1. Comparison of the flow stress obtained from the inverse analysis in the tabular form and calculated from equation (1) with coefficients in table 1 is shown in figure 2. The average error of the inverse analysis was 10%, therefore, in the present work the true stress – true strain curves in a tabular form were implemented into the Abaqus software.

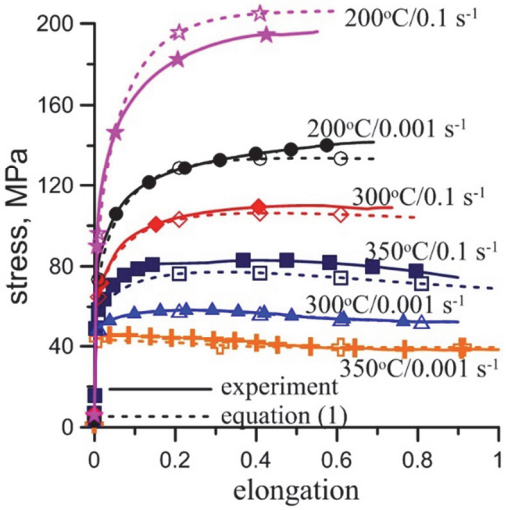

Fig. 2. *Flow stress obtained from the inverse analysis in a tabular form (solid line and filled symbols) and calculated from equation (1) with coefficients given in table 1 (dashed line and open symbols).*

Anisotropy coefficients were determined in the tensile tests and their values are given in table 2. Design of the stamping process requires evaluation of the tendency of the material to cracking. It is particularly important for magnesium alloys, which are characterised by a narrow window of good workability. The forming limit diagram (FLD) for the AZ31 alloy was determined using Nakazima test in the temperature range 20°C – 350°C. Details of the experiment are given in (Ambroziński et al., 2016). Limit curves were approximated by liner functions (figure 3) and these functions were implemented into the Abaqus software.

Table 2. Coefficients of anisotropy at different temperatures.

100 °C	200 °C	300 °C
r_0= 1.91	r_0= 1.9	r_0= 1.138
r_{45}= 2.40	r_{45}= 2.11	r_{45}= 0.994
r_{90}= 3.66	r_{90}= 2.92	r_{90}= 0.943

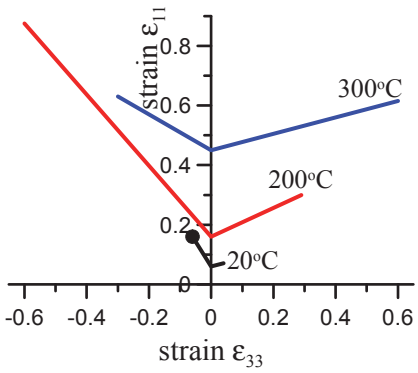

Fig. 3. Forming limit curves for the AZ31 alloy determined in the Nakazima test.

3. STAMPING PROCESS

Using currently available commercial equipment the Mg alloy sheets can be produced up to 600 millimeters wide with a thickness range of 1.5 mm to 6 mm. Through careful selection of alloy composition these alloy sheets are laser weld-able at a rate of 40 meters per minute. In order to make sheets more resistant to corrosion, a commercialized zinc coating process is applied. These sheets can be used to prepare blanks for further stamping process.

Stamping is the main technological process used for manufacturing automotive parts made of strips with the thickness below 2 mm. This process has many advantages among which the following should be mentioned:

- High efficiency
- Reasonably low costs
- Possibility of improvement of the stiffness of products by bending and making reinforcements in the form of stiffness naps (pre-stamped parts).

Majority of car body parts responsible for the safety of passengers are now made of Advanced High Strength Steels (AHSS). Increased strength of these steels allows to decrease weight of the vehicles (Hofmann et al., 2009). Stamping of AHSS parts is performed at room temperature. Martensitic steels, which are stamped at elevated temperatures, are an exception.

As it has already been mentioned workability of magnesium alloys at room temperature is very low and stamping of this material is performed in the temperature range 250°C – 350°C. The objective of the present work was to evaluate possibility of substitution of the steel part by the one made of AZ31 alloy. Expected decrease of the mass of the part is obvious.

3.1. Selection of the part

The bracket used as a support of the driving wheel was selected as a part for investigation. Figure 4 shows the whole support of the driving wheel with marked location of the investigated bracket. This bracket is now made of the construction steel strip with the thickness of 1.2 mm. Investigation was divided into two parts. The first part was focused on the analysis of the stiffness of the bracket made of AZ31 comparing to the steel bracket. Necessary changes in the construction of the bracket needed to obtain required stiffness were considered. In the second part of the investigation numerical simulations were used to evaluate possibility of manufacturing of the bracket by hot stamping.

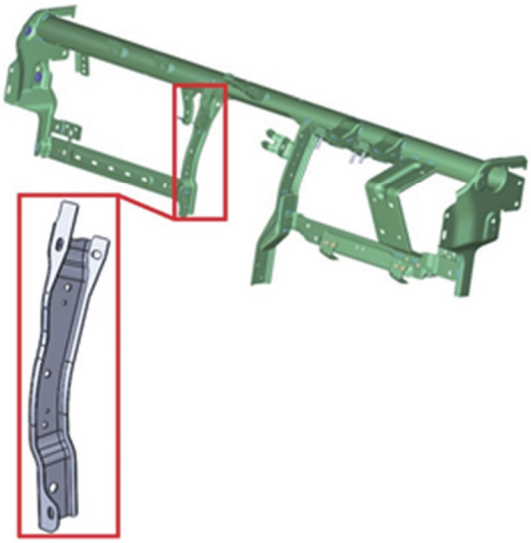

Fig. 4. View of the whole support of the driving wheel with marked location of the investigated bracket.

3.2. Design of the part

Steel part can be substituted by the Mg alloy part only when the latter fulfills criteria concerning stiffness of the construction. Numerical simulations were performed to evaluate the stiffness. Loads used to analyse the stiffness are shown in figure 5. Simulations of the bending of the bracket were performed and stiffness of the bracket made of the two materi-

als was compared. As expected, when the shape was not changed bending of the Mg alloy bracket was much larger. Thus, the following changes in the construction were proposed:

- Increase of the strip thickness to 1.8 mm; it still allowed for 77% decrease of the weight comparing to the steel bracket.
- Adding of reinforcement in the form of stiffening naps (pre-stamped parts) along the bracket.

step equal to the half of the domain size and by dividing the step by half at each iteration. Only slight improvement 52.8% comparing to the previous result was obtained for D = 7.13, R = 0.2 and H = 5.0 mm. This result was discussed with the technologists and the decision was made to put larger weight to the objective function Φ_2. Additionally

Fig. 5. *Illustration of the numerical test performed to evaluate stiffness of the bracket.*

Cross section of the bracket with the stiffening element is shown in figure 6a. Stiffness of the bracket depends strongly on the dimensions of the cross section, in particular on the depth of the naps H. On the other hand an increase of H may lead to difficulties with manufacturing the part and to the increase of the tool costs. Therefore, the optimization task was formulated with the design variables D, R and H and with the constraints due to technological limitations:

$$\begin{aligned} \Phi_1 &= \min\left[b(D,R,H)\right] \\ \Phi_2 &= \min(H) \end{aligned} \tag{2}$$

under constraints:

$$\begin{aligned} R &> t \\ D &< 0.5w - R \end{aligned} \tag{3}$$

where: Φ - objective function, t – thickness of the strip, w – width of the bracket, b – bending of the bracket.

Optimization was performed using variant method. At the first approximation the search domain was constrained to three values of each variable: D = 7.4, 9.9 and 12.4 mm; R = 0.2, 1.2 and 2.2 mm; H = 5.2, 6.2 and 7.2 mm. Objective unction was represented by the per cent decrease of b comparing to the steel bracket. Maximum improvement of 52.5% was obtained for D = 7.4, R = 0.2 and H = 5.2 mm. Following this the steepest gradient descent method was applied. Minimum of the objective function (2) was searched along eight directions beginning with the

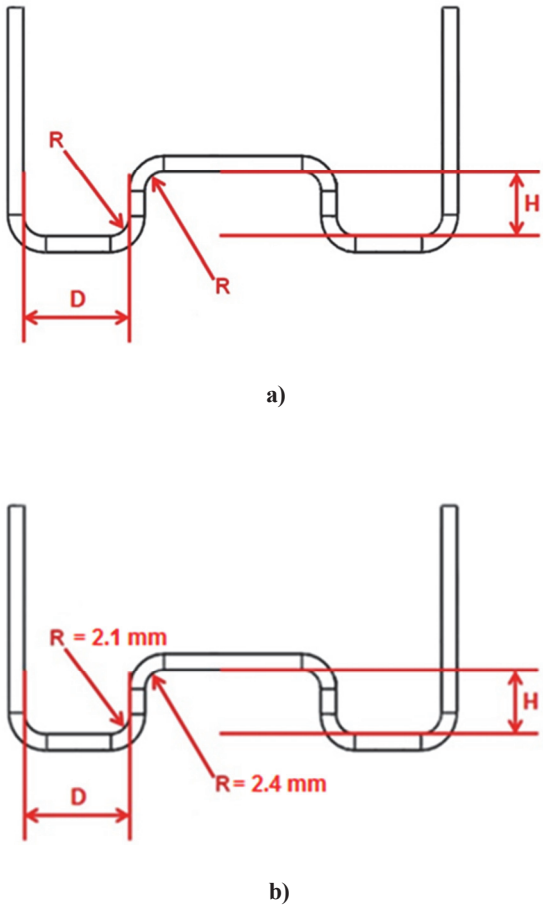

Fig. 6. *Cross section of the new construction bracket with equal radiuses (a) and with different radiuses on the external and internal parts. Optimal values of radiuses are given in figure b.*

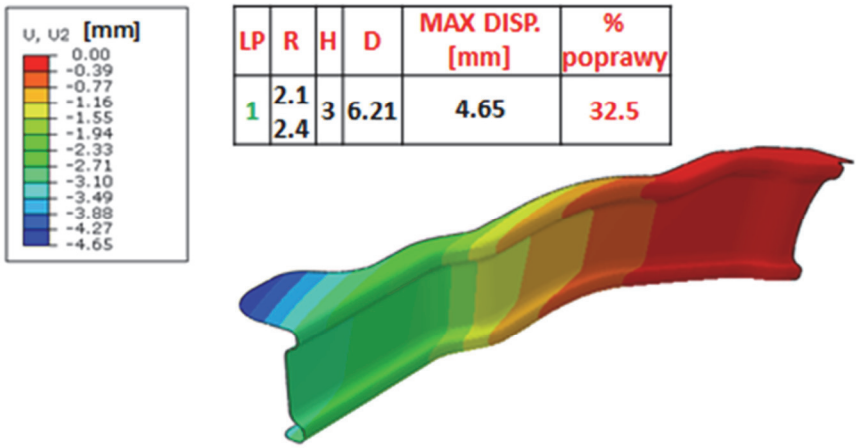

Fig. 7. *View of the optimal bracket with calculated distribution of displacements.*

design variable R was allowed to have different value for the external and internal part of the cross section. Optimization was repeated and the improvement of 32.5% was obtained for $D = 6.21$, $R_1 = 0.21$, $R_2 = 0.24$ and $H = 3.0$ mm. View of the optimal bracket with calculated distribution of displacements is shown in figure 7. It should be emphasized that this optimum, although characterised by smaller improvement of the stiffness (32.5%) comparing to the previous one (52.8%), was obtained for slightly larger radiuses R_1 and R_2 and for much lower depth H, what is advantageous for the technological process.

3.3. Simulation of stamping process

Simulations of stamping of the optimal part described in section 0 was performed next. The boundary conditions were defined to reproduce as closely as possible the stamping process carried out on the laboratory press, see figure 8. In this process the blank was heated by the heat transferred from the die. Simulation of the temperature distribution in the blank was performed first and the results were compared with the measurements using infer red camera and thermocouples welded to the blank. Locations of thermocouples are shown in figure 8b. Calculated distribution of the temperature in the blank is compared in with the measurements using infra-red camera. Good agreement between measurements and calculations was obtained.

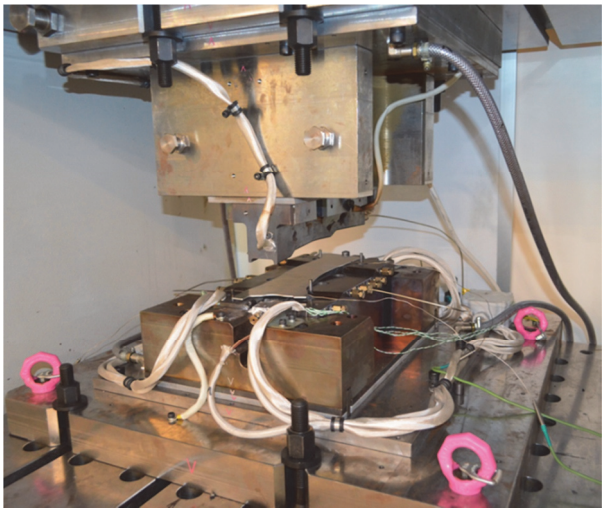

a)

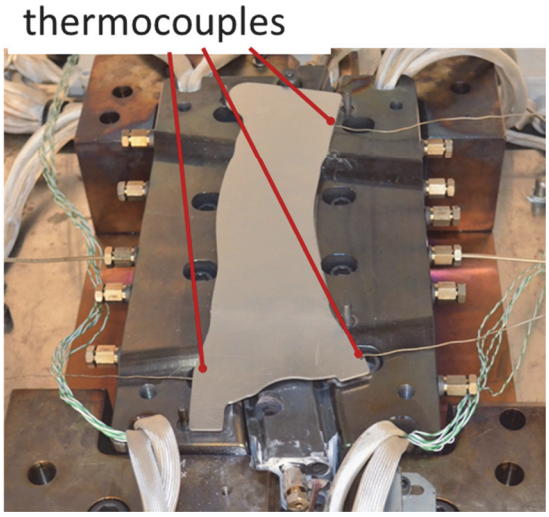

b)

Fig. 8. *View of the press on which the stamping process was performed (a) and locations of thermocouples in the blank (b).*

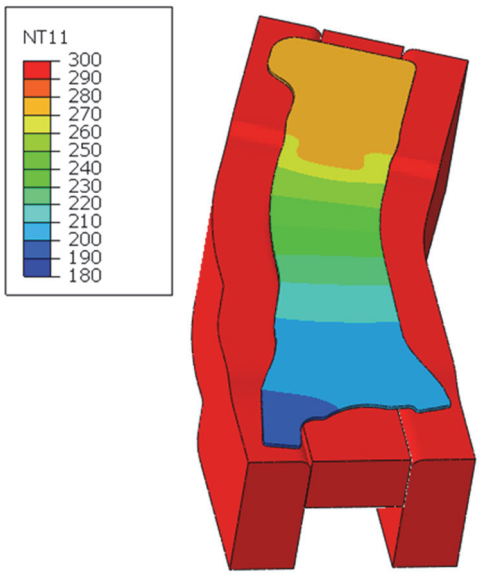

a)

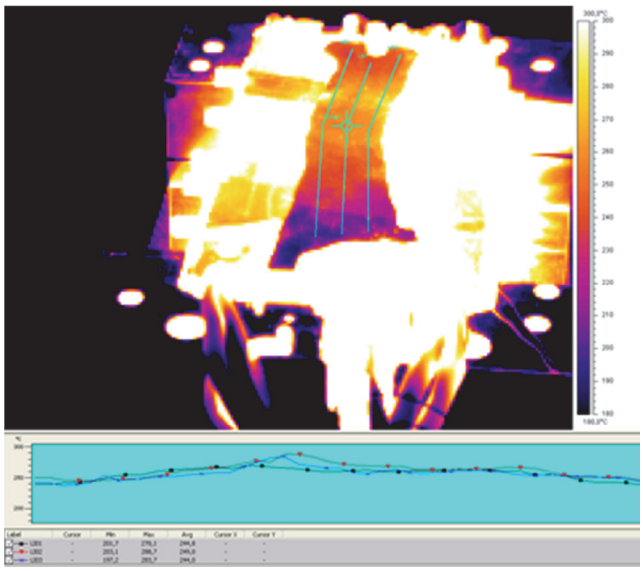

b)

Fig. 9. *Temperature distribution in the blank calculated numerically (a) and measured using infra-red camera (b).*

Simulations of stamping were performed for two ram velocities of 2 mm/s and 10 mm/s and for two temperatures 300°C and 350°C. Full set of results is presented in figure 10 – figure 15. Distributions of maximum and minimum principal strains are shown in figure 11 and figure 12. Areas of strain concentrations are seen along the reinforcement and maximum strains occur at the bending of the bracket. Calculated distribution of the thickness is shown in figure 13. The thickness decreases or increases only slightly in almost the whole bracket except the stiffening pre-stamped area where larger thinning is observed. The minimum thickness was obtained in the area of bending of the bracket in the direction, which caused elongation of the material in the stiffening nap. Contrary, in the area of bending in the opposite direction some increase of the thickness occurred.

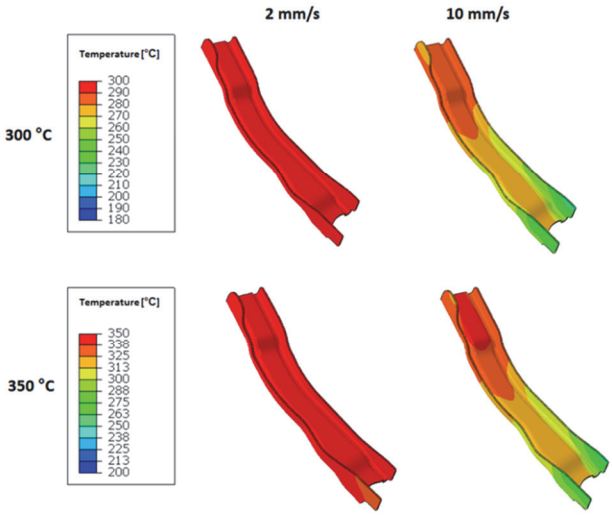

Fig. 10. *Calculated temperature distribution in the bracket after stamping.*

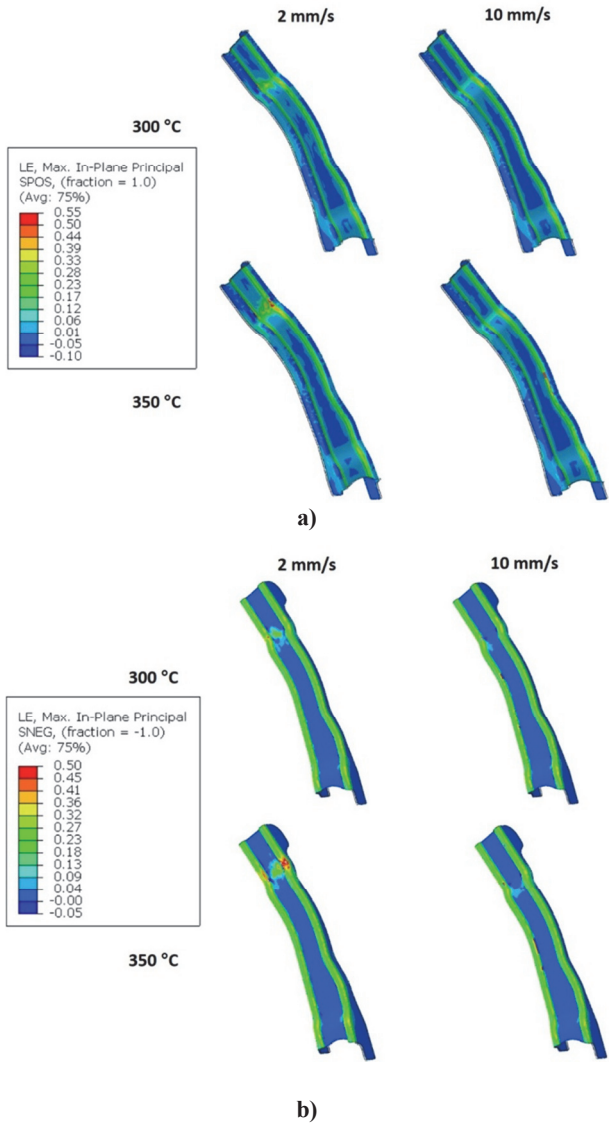

Fig. 11. *Calculated distribution of the maximum principal strain ε_{11} in the bracket, inner surface (a) and outer surface (b).*

The temperature distribution for the slow ram velocity (2 mm/s) was uniform in both cases. Another situation was observed for the higher velocity. When the stamping was made with 10 mm/s the temperature in the bracket was inhomogeneous. Higher temperatures were observed on the upper part of the bracket because this localization remains longer in contact with hot tools. The uniform distribution of temperature on the whole surface of the bracket better solution is advantageous from the hot forming process point of view.

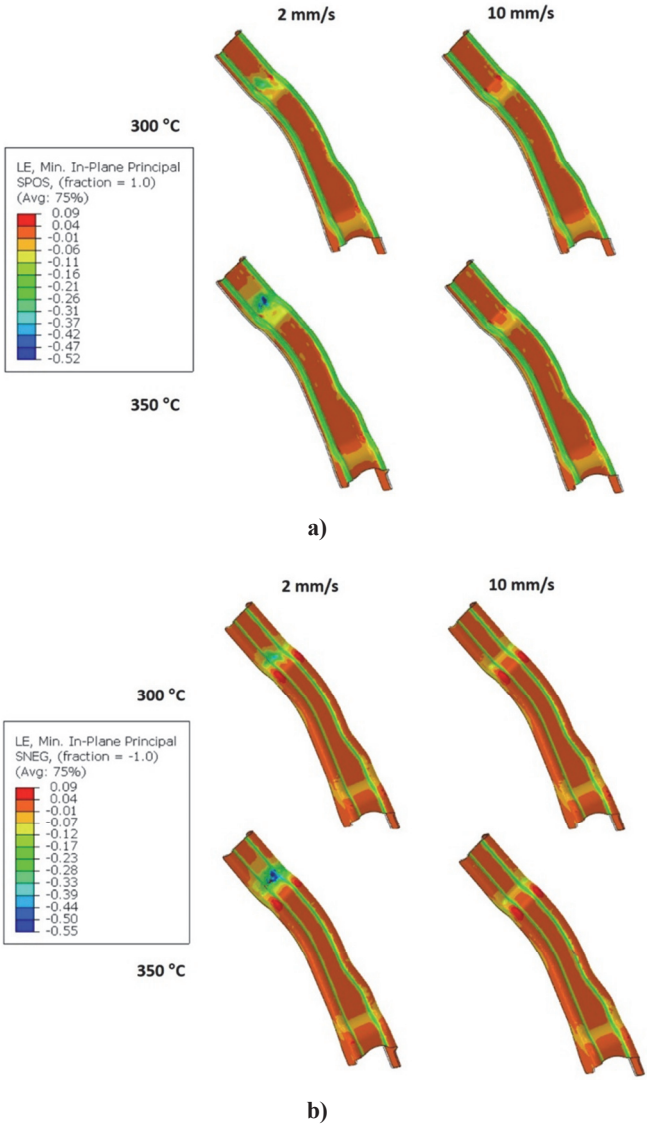

Fig. 12. *Calculated distribution of the minimum principal strain ε_{33} in the bracket, inner surface (a) and outer surface (b).*

Calculated strains were compared with the forming limit diagram shown in figure 3 for the die velocity 2 mm/s (a) and 10 mm/s (b). Strains obtained for different temperatures are distinguished by colours. Coefficients calculated as the ratio between the local strain and the limiting strain at given

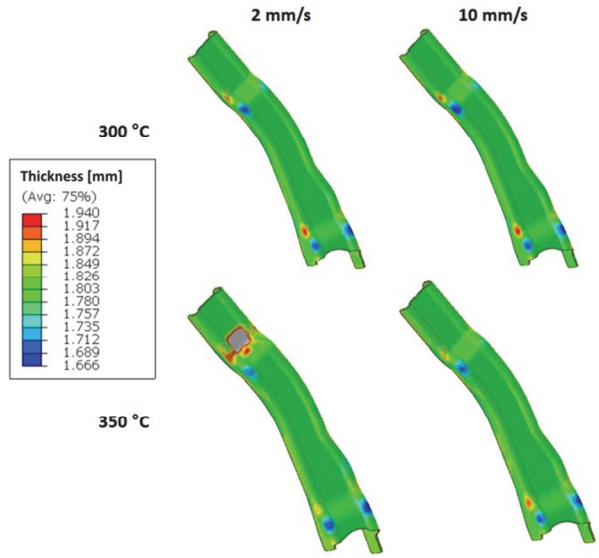

Fig. 13. *Calculated distribution of the thickness.*

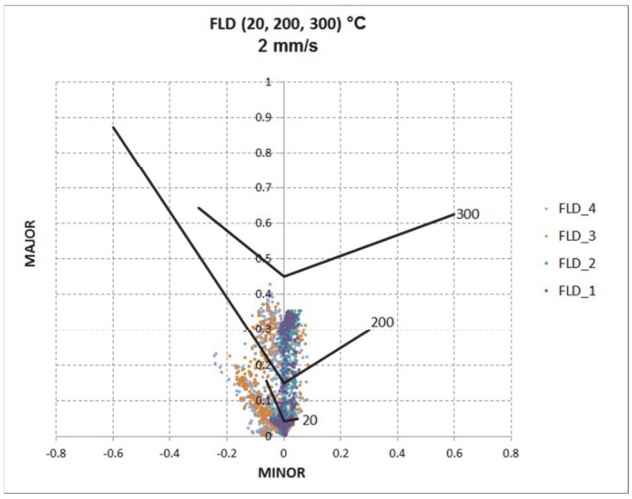

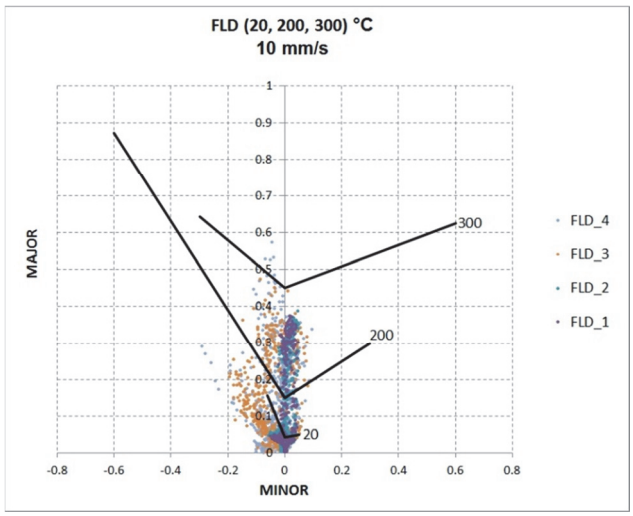

Fig. 14. *Calculated strains compared with the forming limit diagram for the die velocity 2 mm/s (a) and 10 mm/s (b).*

temperature and die velocity. Distribution of this coefficient in the bracket is shown in figure 15.

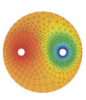

Maximum probability of fracture (0.53) was obtained for the die velocity of 10 mm/s and temperature 300°C and it was localized in the lower part of the bracket in the stiffening pre-stamped area. This concentration was located in the similar area for the die velocity 2 mm/s. Analysis of all the results presented in this section shows that manufacturing of the bracket with reinforcement shown in figure 7 is possible and that decrease of the thickness is acceptable and the strains are below the limiting strains.

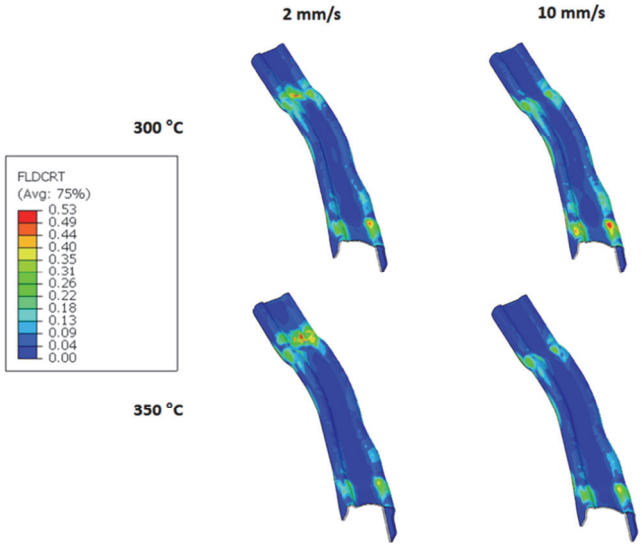

Fig. 15. *Coefficient representing probability of fracture and calculated as ratio between the local strain and the limiting strain at given temperature and die velocity.*

4. CONCLUSIONS

Analysis of the possibility of substitution of steel part in the car body by the one made of AZ31 alloy was performed. Bracket in the support of the steering wheel shown in figure 4 was selected for the analysis. Two criteria had to be fulfilled: i) stiffness of the Mg alloy part could not be lower than that of the steel part, ii) Manufacturing of the part has to be possible without. Numerical simulations allowed to draw the following conclusions:

Thickness of the strip has to be increased to 1.8 mm comparing to 1.2 mm for the steel bracket. It still allows for 77% decrease of the weight for the former part.

Additional reinforcements in the form of stiffening naps (pre-stamped area) have to be added along the bracket. The shape of this reinforcements was designed using optimization with the maximum stiffness and minimum depth used as the objective function.

Numerical simulations of stamping of the optimal bracket showed that the decrease of the thickness is within of acceptable limits and that the strains are below the limiting strains.

ACKNOWLEDGEMENTS

The research was financed by the NCBiR (the National Centre of Research and Development) within the frames of the research project no. PBS1/A5/29/2013.

REFERENCES

Ambroziński, M., Rauch, Ł., Paćko, M., Gronostajski, Z., Kaczyński, P., Jaśkiewicz, K., Krawczyk, J., 2016, Komputerowe wspomaganie projektowania procesu tłoczenia w podwyższonych temperaturach na przykładzie wytwarzania elementu ze stopu magnezu AZ31 dla przemysłu motoryzacyjnego, *Mechanik*, 89, 59-62 (in Polish).

Blawert, C., Hort, N., Kainer, K.U, 2004, Automotive applications of magnesium and its alloys, *Transactions of the Indian Institute of Metals*, 57, 397-408.

Hadasik, E. Kuc, D. Niewielski, G. Śliwa, R., 2009, Rozwój stopów magnezu do przeróbki plastycznej, *Hutnik-Wiadomości Hutnicze*, 76, 580-584 (in Polish).

Hofmann, H., Mattissen, D., Schaumann, T.W., 2009, Advanced cold rolled steels for automotive applications, *Steel Research International*, 80, 22-28.

Kawalla, R., Oswald, M., Schmidt, C., Ullmann, M., Vogt, H.-P., Cuong, N.D., 2008a, New technology for the production of magnesium strips and sheets, *Metalurgija*, 47, 195-198.

Kawalla, R., Ullmann, M., Oswald, M., Schmidt, C., 2006, Properties of strips and sheets of magnesium alloy produced by casting-rolling technology, *Proc. 7th Int. Conf. on Magnesium Alloys and Their Applications*, ed., Kainer, K.U., Dresden, 364-369.

Kawalla, R, Lehmann, G., Ullmann, M., Vogt, H.-P., 2008b, Magnesium semi-finished products for vehicle construction, *International Journal of Advanced Manufacturing Technology*, 8, 93-101.

Kuc, D., Pietrzyk, M., 2010, Physical and numerical modelling of plastic deformation of magnesium alloys, *Computer Methods in Materials Science*, 10, 130-142.

Kuc, D., Hadasik, E., Bednarczyk, I., 2012, Plasticity and microstructure of hot deformed magnesium alloy AZ61, *Solid State Phenomena*, 191, 101-108.

Kuc, D., Hadasik, E., Schindler, I., Kawulok, P., Sliwa, R., 2013, Characteristics of plasticity and microstructure of hot forming magnesium alloys Mg-Al-Zn type, *Archives of Metallurgy and Materials*, 58, 151-156.

Kuc, D., Hadasik, E., Mrugała, A., 2014, Plasticity and microstructure of magnesium-lithium alloys, *Proc. Conf. METAL*, Brno, e-book.

Kulekci, M.K., 2008, Magnesium and its alloys applications in automotive industry, *International Journal of Advanced Manufacturing Technology*, 39, 851-865.

Musfirah, A.H., Jaharah, A.G., 2012, Magnesium and aluminum alloys in automotive industry, *Journal of Applied Sciences Research*, 8, 4865-4875.

Sameer Kumar, D., Tara Sasanka, C., Ravindra, K., Suman, K.N.S., 2015, Magnesium and its alloys in automotive applications, *American Journal of Materials Science and Technology*, 4. 12-30.

Sellars, C.M., McTeggart, G, 1972, Hot Workability, *International Metals Reviews*, 17, 1-24.

Szeliga, D., Gawąd, J., Pietrzyk, M., Kuziak, R., 2005, Inverse analysis of tensile tests, *Steel Research International*, 76, 807-814.

Ullmann, M., Oswald, M., Gorelova, S., Kawalla, R., Vogt, H.P., 2012, Strip rolling technology of magnesium alloys, *Steel Research International*, Spec. issue 14th Metal Forming Conf., 855-858.

WSPOMAGANE KOMPUTEROWO PROJEKTOWANIE PROCESU WYTWARZANIA ELEMENTU NADWOZIA SAMOCHODU ZE STOPU MAGNEZU

Streszczenie

Ocena możliwości zastąpienia stalowej części nadwozia samochodu przez część zrobioną ze stopu magnezu była głównym celem pracy. Jako przykład do analizy wybrano wspornik w układzie kierowniczym. Dla oceny możliwości zastosowania części ze stopu magnezu przyjęto dwa kryteria: i) sztywność tej części nie może być niższa niż sztywność części stalowej, ii) Wytworzenie części w procesie tłoczenia musi być możliwe. Celem badań było zaprojektowanie kształtu wspornika, który spełniałby przedstawione kryteria. Wykorzystując metody optymalizacji zaprojektowano nowy kształt wspornika ze stopu magnezu. Za kryterium optymalizacji przyjęto maksimum sztywności wprowadzając minimum głębokości przetłoczenia jako ograniczenie technologiczne. Wymiary wspornika były zmiennymi decyzyjnymi. Wykonano symulacje numeryczne tłoczenia wspornika o optymalnym kształcie. Wyniki symulacji wykazały, że pocienienie materiału mieści się w dopuszczalnych granicach i że odkształcenia w całej części są poniżej odkształceń granicznych. Projekt wspornika, który może być bezpiecznie wytwarzany metodą tłoczenia, jest głównym osiągnięciem pracy.

Received: July 20, 2016
Received in a revised form: November 9, 2016
Accepted: December 16, 2016